

# Effects of the wildfires in August 2021 on the air quality of Athens through a numerical simulation

Tobias Osswald<sup>A,\*</sup> , Carla Gama<sup>A</sup>, Ana Patrícia Fernandes<sup>A</sup>, Diogo Lopes<sup>A</sup> , Vassiliki Varela<sup>B</sup> and Ana Isabel Miranda<sup>A</sup>

For full list of author affiliations and declarations see end of paper

**\*Correspondence to:**

Tobias Osswald  
CESAM and Department of Environment  
and Planning, University of Aveiro,  
3810-193 Aveiro, Portugal  
Email: [tobiasosswald@ua.pt](mailto:tobiasosswald@ua.pt)

## ABSTRACT

**Background.** Air quality deteriorates significantly during wildfire events, which poses a risk for the health of affected human populations. The Mediterranean Basin was strongly impacted by wildfires during the 2021 fire season, particularly in Greece. **Aims.** This work aims at estimating the impact of the Greek wildfires of August 2021 on the air quality in Athens. **Methods.** The numerical modelling system WRF-APIFLAME-CHIMERE, which comprises a meteorological model, a smoke emissions model and a chemical transport model, was employed in estimating the hourly three-dimensional distribution of particulate matter (PM), CO and O<sub>3</sub> concentrations during the wildfires. The performance of the modelling system was evaluated by comparing modelled results with air quality observations and atmospheric optical depth measurements. **Key results.** Good agreement between measured data and model results was found, with results obtained with a higher-resolution computational grid performing the best. **Conclusions.** The calculated values indicate concerning hourly and daily levels of air pollution, above the limit values for human health protection, during the analysed days within and around Athens. **Implications.** The results highlight the importance of implementing a strategy for human health protection during wildfire events affecting populated areas. This modelling approach could be a basis for a smoke forecasting system.

**Keywords:** atmospheric pollution, carbon monoxide, human health, ozone, particulate matter, smoke modelling, wildfire emissions, wildland–urban interface.

## Introduction

Fire activity around the Mediterranean basin has been increasing over the past years and the burned area in some countries is expected to increase on average by 10% a decade in some countries because of climate change (Dupuy *et al.* 2020). Allied to this are the lack of adequate forest management, which has led during the last decades to the conversion of native oak forests into non-native tree plantations, increasing the risk of large-scale forest fires, and the abandonment of rural areas, which may render the situation even worse as fields and forests are left untended, posing a significant fire risk (Corona *et al.* 2015).

The effects of wildfires are not limited to the massive economic and human losses that are caused directly through the action of flames. Smoke is also a most disturbing consequence of wildfires, with the release of large amounts of gaseous and particulate pollutants into the atmosphere (e.g. Fernandes *et al.* 2022; Xu *et al.* 2022) that strongly impact human health (e.g. Sebastião *et al.* 2019; D'Evelyn *et al.* 2022) and impair visibility (Valente *et al.* 2007). The World Health Organization (WHO), aware of the health effects of smoke from wildfires, provides air quality guidelines for wildfire events to protect the population (WHO 1999), particularly in the wildland–urban interface (WUI) owing to the high risk of human exposure (Miranda *et al.* 2008; Ager *et al.* 2019). Exposure to high air pollution levels during wildfire events can lead to a wide range of adverse health outcomes, including increases in respiratory morbidity

Received: 6 July 2022

Accepted: 29 July 2023

Published: 31 August 2023

**Cite this:**

Osswald T *et al.* (2023)  
*International Journal of Wildland Fire*  
32(11), 1633–1645. doi:[10.1071/WF22148](https://doi.org/10.1071/WF22148)

© 2023 The Author(s) (or their employer(s)). Published by CSIRO Publishing on behalf of IAWF. This is an open access article distributed under the Creative Commons Attribution-NonCommercial-NoDerivatives 4.0 International License (CC BY-NC-ND)

OPEN ACCESS

(Elliott *et al.* 2013; Haikerwal *et al.* 2016; Reid *et al.* 2016; Black *et al.* 2017; Cascio 2018) and negative cardiovascular effects (Haikerwal *et al.* 2015; Yao *et al.* 2016; Wettstein *et al.* 2018). The populations most vulnerable to smoke exposure are the common risk groups (e.g. children and older adults) (Rappold *et al.* 2017; Aguilera *et al.* 2021) and personnel involved in firefighting operations (Miranda *et al.* 2010, 2012; Sebastião *et al.* 2019). Short-term exposure to very high air pollution levels during a fire event can lead to acute health problems, which can be instantaneous irritation of the eyes, nose and throat, and shortness of breath. These symptoms often evolve into headaches, dizziness and nausea, lasting up to several hours.

Greece along with other countries around the Mediterranean suffered unusually high levels of fire activity during the 2021 fire season, and in particular during the first 2 weeks of August. These early August 2021 Greek wildfires were unprecedented in extent, intensity and impacts (Giannaros *et al.* 2022). According to the European Forest Fire Information System (EFFIS; <https://effis.jrc.ec.europa.eu>), five wildfires collectively burnt nearly 94 000 ha, an area that accounts for more than 70% of the 2021 total national burnt area and equals almost three times the 2008–2021 annual average burnt area. Observational evidence indicates that all wildfires showed extreme fire behaviour, characterised by erratic fire spread, massive spotting and the occurrence of pyroconvection (Giannaros *et al.* 2022). Moreover, reports in the media of impressive levels of smoke and ash were supported by measurements of atmospheric pollutants during that period (EEA 2021; Smith 2021), with concentration levels of particulate matter having an equivalent aerodynamic diameter smaller than 10  $\mu\text{m}$  ( $\text{PM}_{10}$ ) well above the threshold defined by the European Ambient Air Quality Directive (2008/50/EC) for the protection of human health, which established 50  $\mu\text{g m}^{-3}$  as the daily limit. Athens was especially impacted because the city and surrounding urban areas, inhabited by 4 million people, were surrounded by two large fires in their vicinity during the first week of August.

Previous studies of extreme wildfire events have successfully employed Chemical Transport Models (CTMs) and satellite data information to achieve high spatiotemporal resolution fields of species concentrations. This method was used by Péré *et al.* (2014) in a case study of an event near Moscow in 2010. They used the Weather Research and Forecasting (WRF) meteorology model coupled with the CHIMERE CTM fed with emissions derived from the Global Fire Assimilation System. The latter uses the satellite-derived Fire Radiative Power (FRP) and vegetation maps to estimate emissions. The authors observed good agreement between satellite observations of Aerosol Optical Depth (AOD) and the model results, whose bias ranged from  $-40$  to 30%. More recently, Turquety *et al.* (2020) used the WRF-CHIMERE system coupled with APIFLAME. This system showed good results in a case study of Portugal in the 2016 fire season for which 5% bias in AOD was

estimated. The authors showed how the state-of-the-art plume rise model as well as the detection of small fires were important factors that allowed reduction of the modelling biases.

The present study aims to better understand the emission and dispersion of smoke during extreme wildfire events, including their impacts on air quality (AQ), using the events surrounding Athens as a case study. For this, biomass-burning emissions are estimated based on a top-down satellite-based methodology (using APIFLAME), and their impact on AQ is assessed based on a modelling approach. The WRF model is used to obtain high spatiotemporal meteorological conditions data while CHIMERE simulates the chemical and physical processes that pollutants undergo within the atmosphere. Evaluation of the modelling system, namely regarding the chosen model parameterisation and input data, was done by comparing results with measurements from AQ monitoring stations and from AERONET sites located within Greece.

In the following section, the case study is described followed by a detailed explanation of the model and its parameterisations. Afterwards the model results are presented, evaluated and discussed. The last section provides the conclusions of this work.

## Data and methodology

The APIFLAME model was used for estimating biomass-burning emissions, while other emissions, meteorology and chemical transport phenomena were handled by the WRF-CHIMERE model and its pre-processors. The system was applied to the case study of Athens during the fires in the beginning of August 2021 with the aim of obtaining multiple air-pollutant concentrations that are representative of wildfire smoke. Particulate matter with an aerodynamic diameter smaller than 10  $\mu\text{m}$  ( $\text{PM}_{10}$ ) and smaller than 2.5  $\mu\text{m}$  ( $\text{PM}_{2.5}$ ) as well as carbon monoxide (CO) are consistently emitted by wildfires and therefore good tracers of smoke (Schneider *et al.* 2021). Thus, these three pollutants were considered the most suitable for assessing the direct impact of wildfires on AQ. Ozone ( $\text{O}_3$ ) is a secondary pollutant, which is produced in the troposphere by photochemical reactions that involve nitrogen oxides ( $\text{NO}_x$ ) and volatile organic compounds (VOCs). As both these components are emitted through biomass burning,  $\text{O}_3$  levels are also expected to be influenced by wildfires (e.g. Jaffe and Wigder 2012; Schneider and Abbatt 2022; Yang *et al.* 2022) and was therefore also analysed. The European Ambient Air Quality Directive (2008/50/EC) sets limit or target values (LVs or TVs) for several air pollutants above which considerable health impacts are expected. For  $\text{PM}_{10}$ , the daily mean should not exceed 50  $\mu\text{g m}^{-3}$  LV. For  $\text{O}_3$  and CO, the values for the protection of human health are defined for the maximum daily 8-h mean and are 120  $\mu\text{g m}^{-3}$  TV and 10  $\text{mg m}^{-3}$  LV respectively.

## Case study

In the beginning of August 2021, several wildfires broke out in the Greek regions of Attica, Euboea, Ilia, Messinia and Lakonia and burnt for several days. According to Giannaros *et al.* (2022), these extreme wildfires were associated with meteorological conditions that, on the one hand, contributed to bringing fuels to a critically flammable condition that could support intense burning (also due to the warm and dry conditions that prevailed during the months preceding August 2021), and, on the other hand, created a mesoscale environment conducive to the development of pyroconvection. Surface weather conditions were marked by a heat wave peaking at 40–45°C by the end of July that contributed to pushing relative humidity levels to below 20% in all fire-affected regions (Giannaros *et al.* 2022). Synoptic conditions were marked by the breakdown of a strong upper-level ridge that occurred as an upper-air long-wave trough moved into the southeast Mediterranean. This led to the advection of moist mid-level air over the very dry lower troposphere of the fire-affected regions, leading to the development of pyroconvection (Giannaros *et al.* 2022). Fig. 1 shows a satellite image of the smoke produced during these wildfires as acquired by the Visible Infrared Imaging Radiometer Suite (VIIRS) on Suomi National Polar-orbiting Partnership (NPP).

Five wildfires collectively burnt nearly 94 000 ha, an area that accounts for more than 70% of the 2021 total burnt area. Table 1 shows fire activity information for these five

largest wildfires. This information is based on data provided by the Hellenic Fire Service, on data published by Giannaros *et al.* (2022) and on information from Xanthopoulos *et al.* (2022).

According to the Hellenic Fire Service (2021), a wildfire started 100 km to the north of the city of Athens on Evia Island at 17:11 hours on 3 August and continued to burn until 17 August. This resulted in ~51 200 ha burned (40% of the total during that fire season in Greece) as estimated by the European Forest Fire Information System Burnt Area satellite product (EFFIS 2022). Another wildfire started directly to the northeast of Athens on 3 August at 13:22 hours, ending on 12 August, with a rekindling on 5 August, resulting in 8400 ha burned (Hellenic Fire Service 2021).

Almost simultaneously, three other aggressive fires had started in the Peloponnese, the most threatening being the one in the prefecture of Ilia. According to Xanthopoulos *et al.* (2022), they became very large: the fire in Ilia reached 15 000 ha, the fire in Messinia 5100 ha, and the fire in Lakonia (Mani) 10 100 ha, devastating both forest and agricultural lands.

Other significant fires were detected through their FRP signatures in western Greece and in neighbouring countries during that period (Giglio *et al.* 2021). Residents reported heavy deposition of ash in the city and authorities advised the population to stay indoors or use respiratory masks otherwise (Smith 2021).

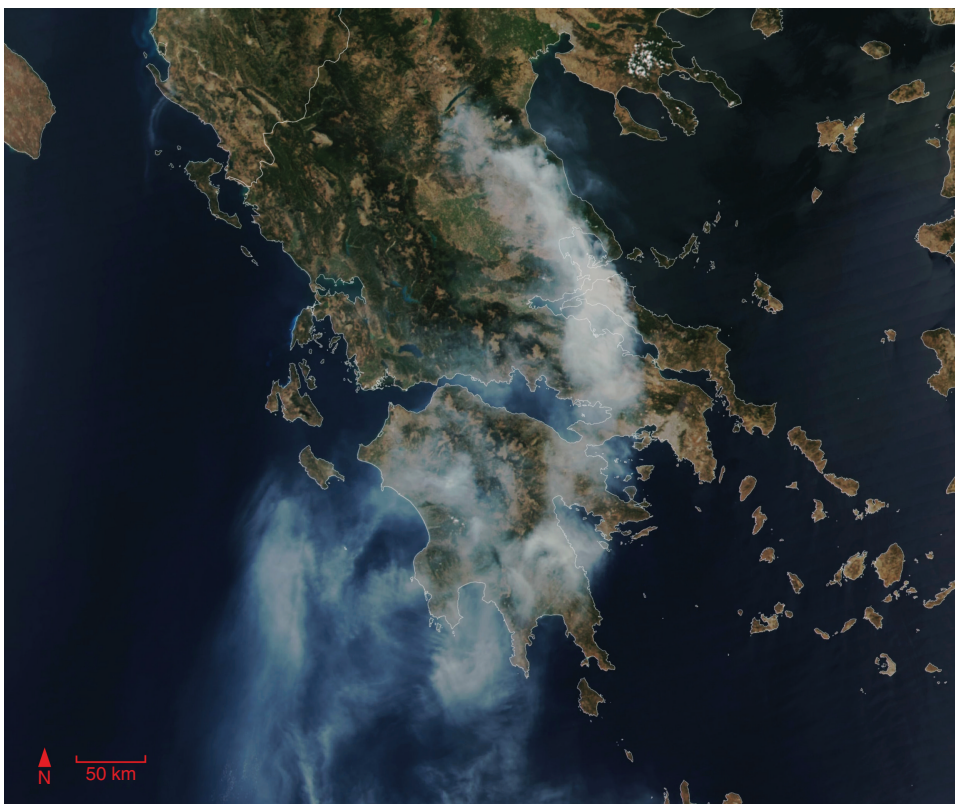


**Fig. 1.** Wildfire in Greece on 8 August 2021 (by NASA Earth Observatory, <https://earthobservatory.nasa.gov/images/148682/fire-consumes-large-swaths-of-greece>, public domain).

**Table 1.** Fire activity information.

Region	Ignition time (date, time (hours))	Ignition location (°N, °E)	Burnt area (ha)	Comments
Attica (near Athens)	3 August, 13:22	38.1317, 23.8044	8400	The fire started 18 km north of the centre of Athens, near a settlement called Varympompi, one of the wildland–urban interface areas that exist around the city
Euboea (Evia Island)	3 August, 17:11	38.7940, 23.3242	51 200	Included areas recognised as landscapes of high quality and biotopes characterised by Natura and Cortine
Lakonia	3 August, 10:30	36.8472, 22.3885	10 100	Peloponnese Peninsula; forest and agricultural lands
Iliia	4 August, 10:03	37.7016, 21.5747	18 400	
Messinia	4 August, 16:51	37.3251, 21.9410	5100	

## Modelling setup

### APIFLAME

Biomass-burning emissions of trace gases and aerosols during the 2021 Greece wildfires were calculated using the APIFLAMEv2 model (Turquety *et al.* 2020). The estimates are based on pre-processed satellite imagery in the form of the MODIS (Moderate Resolution Imaging Spectroradiometer) burned scars product (MCD64A1), which uses thermal anomalies from active fires and changes in reflectance due to the charring of the vegetation to detect burned regions. This product has a 500 m resolution and is released monthly indicating the estimated day of burning for each detection. For each fire and associated vegetation type, the amount of consumed fuel was calculated, and the corresponding emissions of trace gases and aerosols were derived using a list of emission factors. When modelling the impact of wildfires on AQ at a regional scale, information on the diurnal variability of emissions has been shown to be critical (Rea *et al.* 2016; Turquety *et al.* 2020). In our study, the biomass-burning emissions are distributed throughout the day using a typical wildfire temporal profile. The module also uses the FRP from the MOD14 satellite product, which processes four daily observations at 1 km resolution. Out of these, the daily maximum is used by CHIMERE to calculate the injection height.

### WRF-CHIMERE

The impact of the emissions of wildfires on AQ was quantified based on a modelling approach, using the state-of-the-art CHIMERE model (Menut *et al.* 2021). This model is an open-source multi-scale Eulerian CTM, which includes detailed gas-, aerosol- and cloud-phase chemistry. The chosen MELCHIOR2 chemistry mechanism takes 49 species and 120 reactions into account. Additionally, seven aerosol species are subdivided into 10 size bins, whose chemistry is also considered. CHIMERE can run over a range of spatial scales from the hemispheric to the urban scale (up to  $1 \times 1 \text{ km}^2$ ). It has been widely used for air quality studies in Europe, which has allowed extensive testing and model evaluation over this study region (e.g. Kukkonen *et al.* 2012; Bessagnet *et al.* 2016; Colette *et al.* 2017). WRF is run on the same grid in parallel and feeds CHIMERE with data on meteorological variables such as wind speed, temperature and humidity.

The WRF-CHIMERE system was run between 27 July 2021 and 10 August 2021, providing a 7-day spin-up period to stabilise all simulation variables that may be affected by inaccuracies in the initial conditions before the first fires in the vicinity of Athens started. A fine simulation domain of Athens was nested inside a medium one containing most of Greece, which in turn was nested in a continental domain, resulting in three computational domains with resolutions of 25, 5 and  $1 \text{ km}^2$  (see Fig. 2). The coarser mesh captured phenomena at the level of the Mediterranean Basin with  $95 \times 69$  cells, the intermediate one was positioned around Greece with  $106 \times 81$  cells and the smallest one was

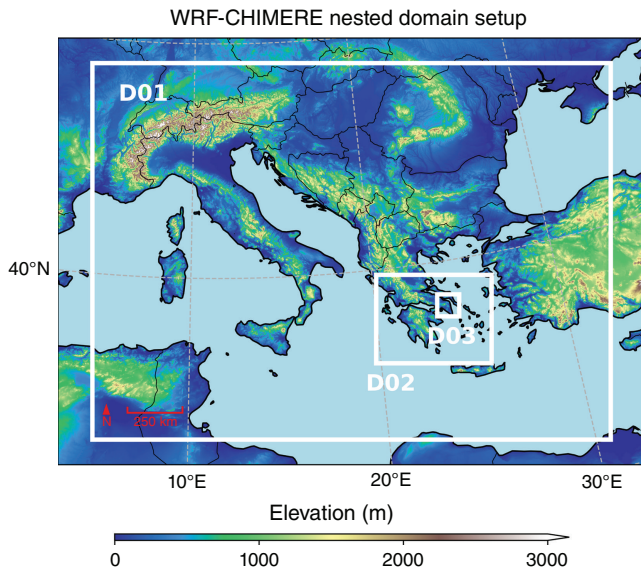


**Fig. 2.** WRF-CHIMERE nested domains used for the simulations plotted over an elevation map of the Mediterranean Basin. D01, coarse domain with 25 km<sup>2</sup> resolution; D02, intermediate domain with 5 km<sup>2</sup> resolution; D03, small domain with 1 km<sup>2</sup> resolution.

composed of 100 × 100 cells over Athens, thus providing a detailed picture of the AQ over the city. The structured hexahedral mesh was created over a Lambert conformal map of the computational domain with 24 cells between the surface and 200 hPa.

Wildfire emissions coming from APIFLAME were redistributed in the vertical direction according to a plume rise profile that assigns 20% of the emissions below the injection height and the remainder around that same height. *Menut et al. (2018)* tested another profile and concluded that no clear differences in performance could be found. The assumption was that strong mixing in the boundary layer quickly disperses the initial shape of the plume, so that its effect would only be relevant at a local scale.

The injection height of the wildfire plume in CHIMERE was calculated according to the parameterisation of *Sofiev et al. (2012)* with a correction of the FRP for the case of large fires as suggested by *Veira et al. (2015)*. The empirical correlation developed by *Sofiev et al. (2012)* was based on the assumption that the wildfire plume rises owing to the heat generated up to a height at which all the energy from the fire has been dissipated. Thus, it depends only on the state of the atmosphere and heat transfer to the air:

$$H_p = \alpha H_{abl} + \beta \left( \frac{FRP}{P_{f0}} \right)^\gamma \exp(-\delta N_{FT}^2 / N_0^2), \quad (1)$$

where  $H_p$  is the plume rise height,  $H_{abl}$  the atmospheric boundary layer height, FRP the fire radiative power,  $P_{f0}$  the reference FRP,  $N_{FT}$  the Brunt–Väisälä frequency of the free troposphere (calculated as the average value of grid cells between  $H_{abl}$  and 300 hPa) and  $N_0$  the reference

Brunt–Väisälä frequency. The other parameters were adjusted to satellite observations for the optimal performance of the model and are set to

$$\alpha = 0.24; \beta = 170 \text{ m}; \gamma = 0.35; \delta = 0.6$$

$$P_{f0} = 10^6 \text{ W}; N_0^2 = 2.5 \times 10^{-4} \text{ s}^{-2}. \quad (2)$$

Values are hourly adjusted based on hourly atmospheric values calculated by WRF-CHIMERE, such as boundary layer height.

In CHIMERE, for cases where  $H_p > 1500$  m, the correction of *Veira et al. (2015)* is applied such that

$$FRP^* = FRP \left( \frac{H_p}{1500} \right)^{0.5}, \quad (3)$$

as *Veira et al. (2015)* considered that MODIS observations tended to underestimate FRP in the cases of high-intensity wildfires owing to the opacity of the smoke to satellites. Another correction is applied in all cases whenever the considered period is between 18:00 and 06:00 hours. During this night-time period, where the boundary layer height tends to be lower, only half of the FRP is considered in the calculation of the plume rise. The next step of the algorithm consists in comparing the obtained value with other estimates. In cases where the atmospheric boundary layer height is larger than the estimated  $H_p$ , the former is used instead. Finally, a lower threshold of 1 km is applied.

In addition to biomass burning, the AQ simulations considered anthropogenic, mineral dust, biogenic and sea salt emissions. Anthropogenic emissions from *EMEP/Centre on Emission Inventories and Projections database (2021)* were processed to obtain hourly fluxes for the different model species (associated with the selected chemical mechanism) and the specific simulation grids. Available time profiles for specific countries were used, as well as spatial proxies such as land use, population density and road network density. Desert dust, marine aerosols and biogenic emissions were estimated by the model during the simulations, taking static datasets and meteorological data into account.

For the AQ simulations, the boundary conditions for the WRF meteorology were obtained from the ERA-5 reanalysis dataset (*ECMWF 2022*). Variables were taken with a horizontal resolution of 30 km and 37 pressure levels between 1000 and 1 hPa, at 6-h intervals. Once these calculations had been performed, the higher resolution data were passed on directly to CHIMERE.

## Observations

Available observations of pollutant concentrations and aerosol optical depth were used to show the ability of the system to model smoke emission and dispersion, and complement model results.

Air quality observations were extracted from the AQ database of the European Environmental Agency (*EEA 2021*) for

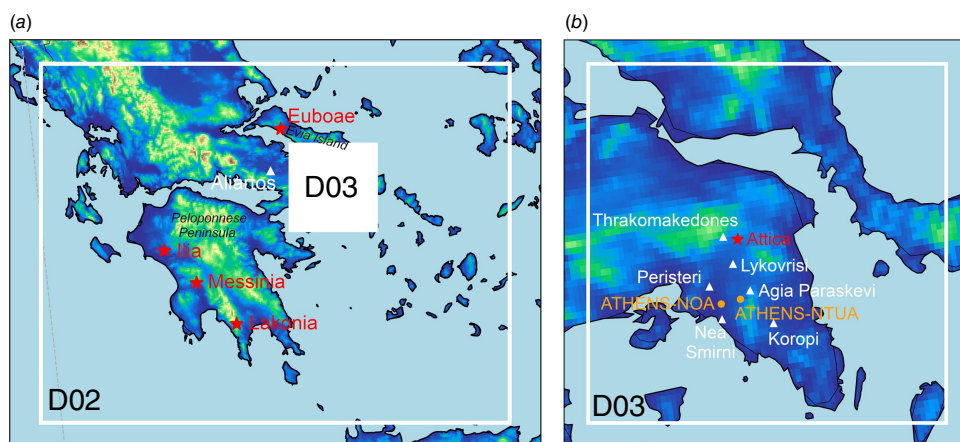


**Fig. 3.** Location of AQ monitoring stations (white triangles) and AERONET sites (orange circles) located within D02 (a) and D03 (b). Ignition locations of the major wildfires, identified in Table 1, are depicted as red stars. Elevation color-scale as in Fig. 2.

the air quality monitoring stations located within D02 and D03, and for the selected pollutants  $PM_{10}$ ,  $PM_{2.5}$ , CO and  $O_3$ .

The selected monitoring stations include only ‘background’ stations, which are more representative of a larger area around them, as opposed to ‘traffic’ or ‘industrial’ stations, which are greatly affected by local phenomena, i.e. sub-grid phenomena for the mesoscale model. Fig. 3 shows the location of the AQ monitoring stations in the D03 finer-resolution domain as well as the Aliartos station, the only station in the database that was recording at the time outside D03 and within D02.

The D03 stations are located in suburban areas except for Nea Smirni and Peristeri, which are within Athens, whereas Aliartos is the only rural station.

Observations of AOD were retrieved from the sites of the Aerosol RObotic NETwork (AERONET; Giles et al. 2019) at the National Technical University of Athens (ATHENS\_NTUA) and the National Observatory of Athens (ATHENS-NOA). AERONET Version 3 AOD Level 1.5 was used, which means data were cloud-cleared and quality controls were applied though a final calibration may not have been applied. Quality-assured Level 2.0 data were not yet available for the period of this study.

## Results and discussion

### Wildfire emissions

For the period studied, emissions from D02 were quantified and can be seen in Table 2. The day with the most activity was 6 August, with a total emission of 19.2 kt PM. In total, 48.5 kt  $PM_{10}$ , 267 kt CO and 6.7 kt  $NO/NO_2$  were released during the studied period. As a comparison, during the wildfires that took place in October 2017 in Portugal, the most devastating over the past decade, 250 kt  $PM_{10}$ , 3500 kt CO and 75 kt  $NO_x$  were emitted according to a detailed study carried out by Fernandes et al. (2022). The authors also showed that satellite-based emission estimates, such as

**Table 2.** Total emissions in D02 domain on each day.

Date	$PM_{10}$	$PM_{2.5}$	CO	$NO_2$	NO
Total emissions (kt)					
3-8-2021	0.55	0.39	2.90	0.01	0.07
4-8-2021	4.15	2.98	22.84	0.09	0.50
5-8-2021	5.44	3.84	33.07	0.10	0.59
6-8-2021	19.20	13.71	104.4	0.40	2.33
7-8-2021	8.72	6.23	45.25	0.18	1.06
8-8-2021	6.30	4.40	34.76	0.12	0.71
9-8-2021	4.15	2.90	23.38	0.08	0.47
Total	48.51	34.46	266.6	0.98	5.73

the ones of APIFLAME, compared well with their own estimates in terms of total values, despite not having a very high spatial resolution.

### Aerosol optical depth

Biomass-burning emissions affect not only the near-surface pollutant concentrations, i.e. what we call air quality, but also the amount of aerosol and gaseous species at higher altitudes. Fig. 4 shows the modelled AOD for the 5-km resolution D02 domain, which is a measure of column-integrated aerosol optical properties, according to model results, between 3 and 6 August 2021.

According to model results, AOD hotspots appear on 4 August, associated with the fire in Evia. As biomass-burning emissions continue in the following days, a plume of AOD is formed and maintained towards the east, with regions reaching  $AOD > 3.0$ . Smaller AOD hotspots are also visible within the Peloponnese Peninsula. On 6 August, an AOD plume appears near Athens due to the fires that broke out in Attica.

Fig. 5 shows the comparison of model results with AOD observations for the two AERONET sites located within the

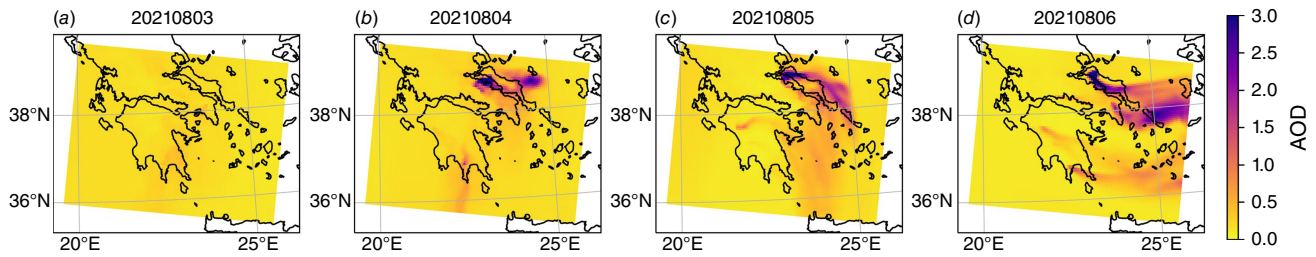


**Fig. 4.** Spatial distribution of the aerosol optical depth (AOD, at 400 nm) within the D02 domain, for days 3-8-2021 (a), 4-8-2021 (b), 5-8-2021 (c) and 6-8-2021 (d) (at 16:00 hours every day).

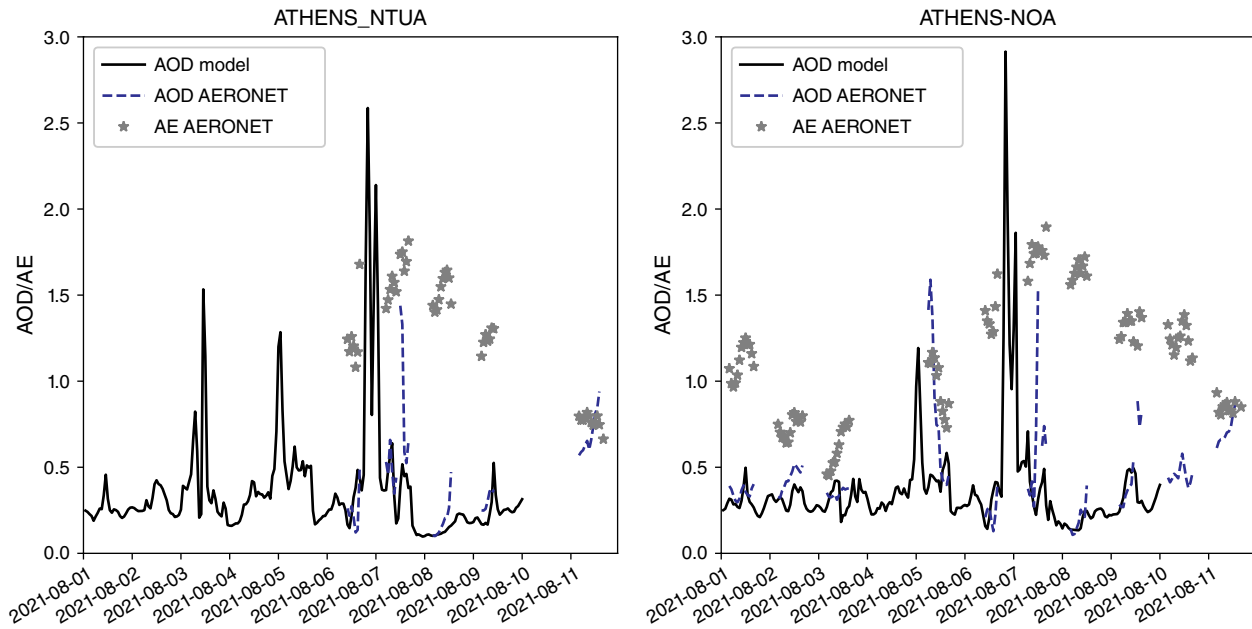


**Fig. 5.** Measured and modelled aerosol optical depth (AOD at 400 nm) and Ångström Exponent (calculated between 380 and 440 nm) at AERONET sites of ATHENS\_NTUA (37.977°N, 23.783°E) and ATHENS-NOA (37.972°N, 23.718°E).

D03 domain. AERONET Ångström exponents (AE; computed from aerosol optical thickness measurements at 380 and 440 nm) were used to estimate aerosol optical thickness at the same wavelength as the model data (400 nm), following Ångström's law. The AE is an indicator of the average aerosol particle size in the atmosphere. An  $AE < 1$  indicates an aerosol size distribution mainly dominated by coarse-mode aerosols (such as dust or sea spray) whereas an  $AE > 1$  usually indicates a size distribution dominated by fine-mode aerosols of effective radius smaller than  $0.5 \mu\text{m}$ , usually associated with urban pollution or biomass burning (Eck *et al.* 1999).

At the location of both AERONET sites, modelled AOD values are maximal in the late afternoon of 6 August (when AOD reaches values above 2.0). AERONET observations show high values of measured optical thicknesses (AOD  $\sim 1.5$ ) associated with large AE ( $1.5 < AE < 2.0$ ) on 7 August. The AERONET observations during 7 August show the influence of the biomass-burning emissions to the total atmospheric aerosol.

## Air quality

Concentrations of  $\text{CO}$ ,  $\text{PM}_{10}$  and  $\text{O}_3$  at the surface were analysed through time-series of maps from the simulations of the 5 and 1 km resolution domains. Concentration snapshots at critical hours from 4 to 9 August 2021 are shown in Fig. 6.

The simulations reveal that on 3 August, a wildfire in the northern urban area of Athens was actively producing a smoke cloud, as seen in Fig. 6. During that day, simulated values at the locations of the monitoring stations (see Figs 7–10) south of Thrakomakedones and north of Koropi exceeded the daily LV for  $\text{PM}_{10}$ . At Lykovrisi, closest to the wildfire, the results indicate an exceedance of twice the daily LV.

The Athens wildfire mostly dies out during 4 August, while emissions from the fire in Evia begin at 01:00 hours according to the model. The smoke is mostly contained over the island until the end of the day. Nonetheless, the

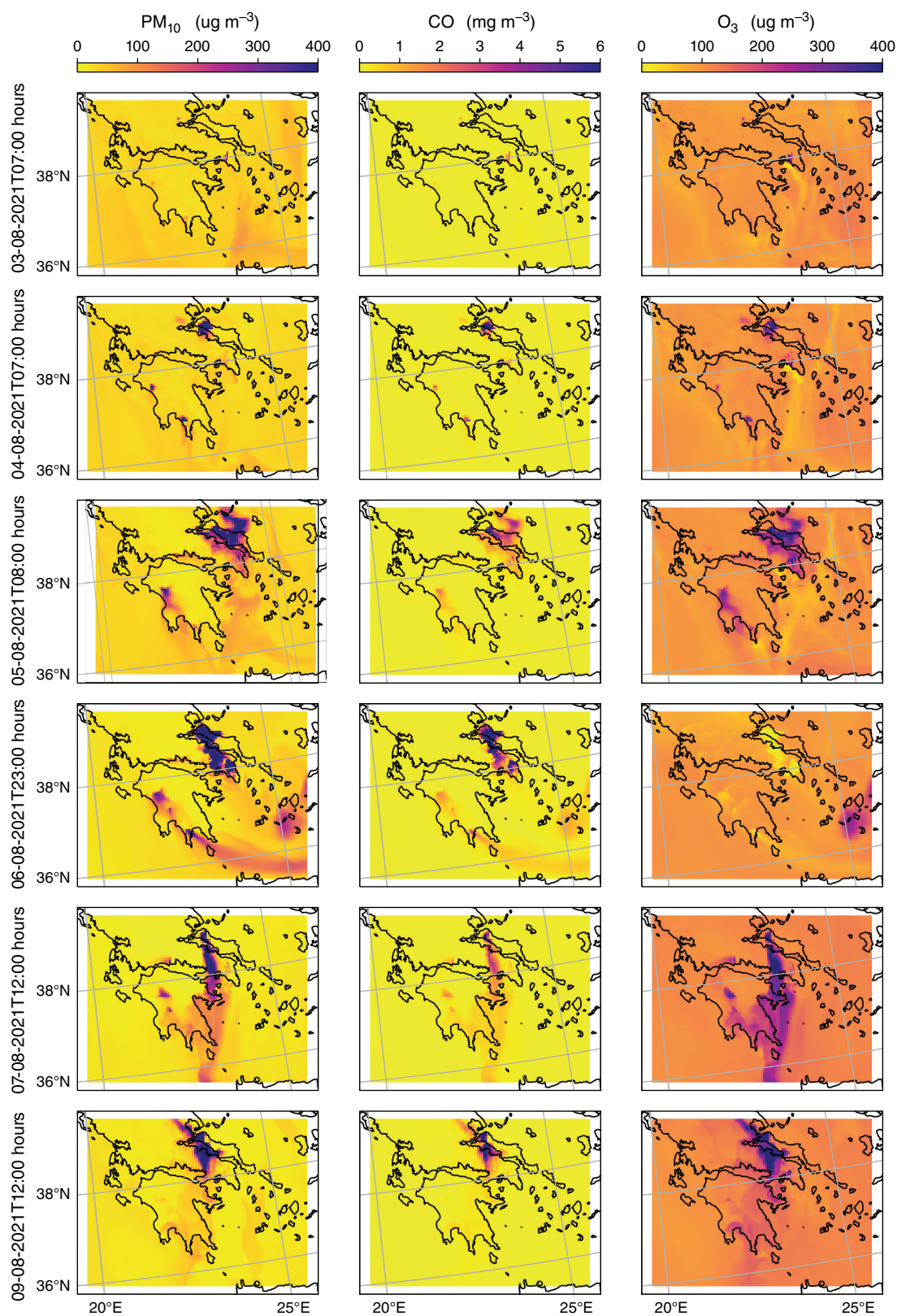


**Fig. 6.** Spatial distribution of the  $\text{PM}_{10}$ , CO and  $\text{O}_3$  concentrations of simulated values at surface level from 3 to 9 August 2021. D03 results are overlaid on the D02 results.

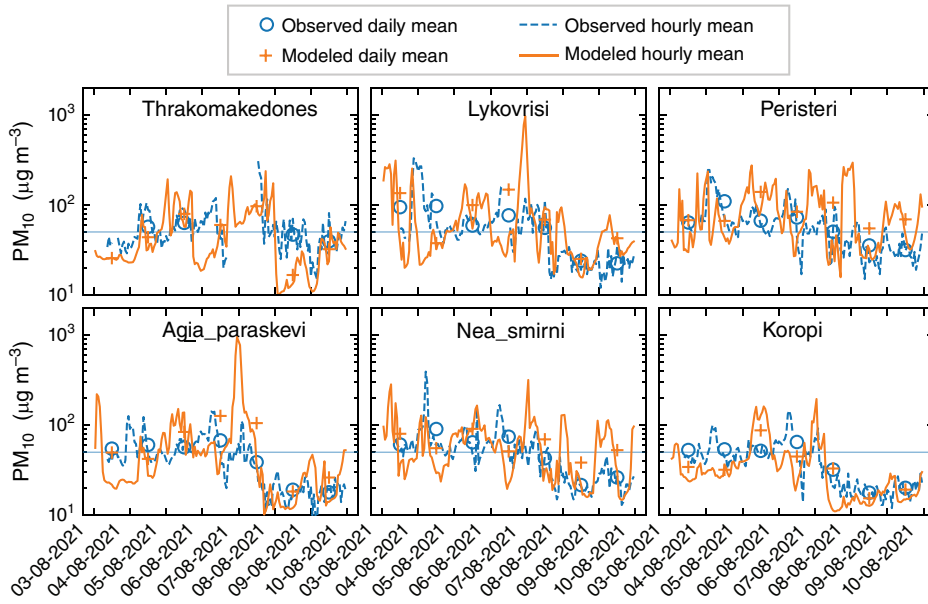


**Fig. 7.** Measured and simulated hourly and daily concentrations of  $PM_{10}$  at monitoring stations in Athens, ordered north to south. The grey line shows the daily LV for the protection of human health ( $50 \mu g m^{-3}$ ).

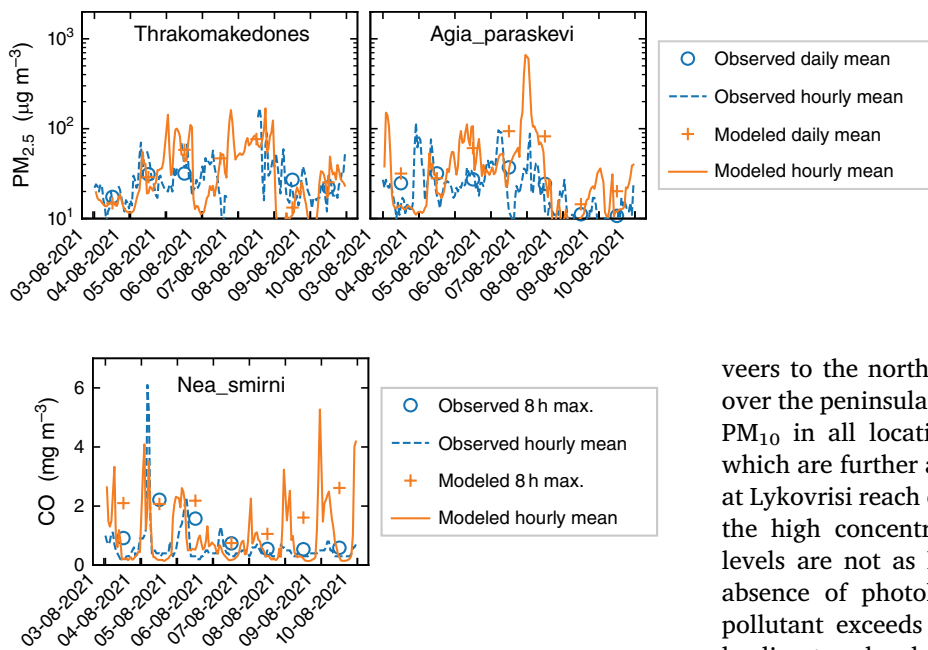


**Fig. 8.** Measured and simulated hourly and daily concentrations of  $PM_{2.5}$  at monitoring stations in Athens, ordered north to south.

**Fig. 9.** Measured and simulated hourly and 8 h maximum concentrations of CO at Nea Smirni, Athens.

locations of Nea Smirni and Peristeri, both urban areas, exceed the  $PM_{10}$  daily LV.

On 5 August, the Athens fire is reactivated and produces, together with the Evia wildfire, a smoke cloud over the peninsula. All locations exceed the daily LV of  $PM_{10}$ ; in particular, Peristeri exceeds twice this value.

Both fires continue to burn throughout 6 August; however, a strong westerly wind during the morning pushes the smoke cloud away from the city. In the afternoon, the wind

veers to the north and smoke from both fires accumulates over the peninsula, leading to exceedances in the daily LV of  $PM_{10}$  in all locations except for Nea Smirni and Koropi, which are further away from the fires. The simulated values at Lykovrisi reach extreme hourly values of  $1152 \mu g m^{-3}$ . As the high concentrations of smoke occur after sunset,  $O_3$  levels are not as high as during the previous day. In the absence of photolysis, the destruction of this secondary pollutant exceeds its production within the smoke cloud, leading to a local concentration minimum.

The wildfire in Evia emits a considerable smoke cloud that reaches the city of Athens. During midday of 7 August, model results show transport by a northerly wind. When the wind was blowing from other directions or with less intensity, this led to periods of less smoke over the city, such as at midday on 9 August. Both simulated values and observations show lower concentrations following the peak of 7 August, with the exception of modelled CO values at Nea Smirni, which exhibit abnormally high values in the simulation. Before 8 August, the performance of the model for CO at Nea Smirni is clearly better. Throughout the simulated period, the CO concentrations in Nea Smirni never exceed the daily 8-h mean LV.

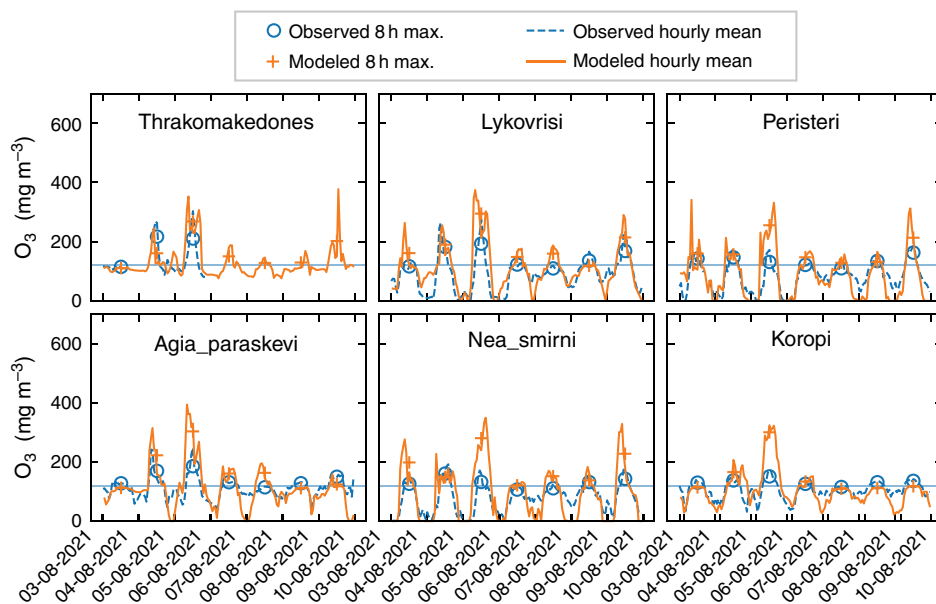


**Fig. 10.** Measured and simulated hourly and 8 h maximum concentrations of O<sub>3</sub> at monitoring stations in Athens, ordered north to south. The grey line shows the maximum daily 8 h mean TV for the protection of human health (120 μg m<sup>-3</sup>).

**Table 3.** Performance metrics definition used for model evaluation.

NMB	$\frac{\sum_{i=1}^N (M_i - O_i)}{\sum_{i=1}^N O_i}$	0 [-∞; +∞]
MFB	$\frac{2}{N} \sum_{i=1}^N \frac{M_i - O_i}{M_i + O_i}$	0 [-∞; +∞]
RMSE	$\sqrt{\frac{1}{N} \sum_{i=1}^N (M_i - O_i)^2}$	0 [0; +∞]
R	$\frac{\sum_{i=1}^N (O_i - \bar{O})(M_i - \bar{M})}{\sqrt{\sum_{i=1}^N (O_i - \bar{O})^2} \cdot \sqrt{\sum_{i=1}^N (M_i - \bar{M})^2}}$	1 [-1; +1]
IOA	$1 - \frac{\sum_{i=1}^N (M_i - O_i)^2}{\sum_{i=1}^N ( M_i - \bar{O}  +  O_i - \bar{O} )^2}$	1 [0; 1]

Optimal value and possible range of values given. O and M are the hourly observations and model results respectively, with the overbar denoting averaging.

### Performance metrics

Five performance metrics were calculated for all the stations of interest using the predictions of both the D02 and the D03 domains. The normalised mean bias (NMB), mean fractional bias (MFB), root-mean-square error (RMSE), Pearson’s correlation coefficient (R) and the index of agreement (IOA). The formula for each is given in Table 3 along with the optimal values followed by the possible range.

The average value of the observations is also provided. The results are given in Table 4.

The D03 domain tends to produce better results, though for some cases D02 has a better performance. This suggests that there is no clear reason to disregard the D02 results altogether.

To evaluate the performance of D02 outside Athens, only the Aliartos station can be used as all other stations in the EEA AQ database were not recording during the period of interest. Its performance metrics are close to those for the remaining

stations. An exception to this is the RMSE for PM<sub>10</sub>, which shows the highest value, or the metrics of O<sub>3</sub>, which are somewhat worse than in other stations available within the D03 domain. Differences can be explained not only by its distance to other stations but also by the fact that it is the only rural station analysed. Moreover, as O<sub>3</sub> is a photochemical pollutant, its production or destruction depend among other variables on temperature and solar radiation. However, temperature and solar radiation are meteorological variables that are affected by the direct feedback of aerosols emitted during wildfires (Péré et al. 2014). However, our simulations do not consider those feedbacks between atmospheric composition and meteorology, which may contribute to poorer model performance in simulating O<sub>3</sub> concentrations.

Despite the limitations identified in the simulation of the chemical processes for O<sub>3</sub>, the IOA shows that this pollutant was better simulated than the others, with IOA values varying between 0.54 and 0.80. There was only one monitoring station with available CO data for the evaluation, with a calculated IOA of 0.37 and 0.52 for D02 and D03, respectively. Except for the Agia Paraskevi monitoring station location, where a simulated peak value was not observed, the hourly performance metrics for PM, for both PM<sub>10</sub> and PM<sub>2.5</sub>, were quite acceptable and it is well known that PM is a difficult pollutant to model when compared with other gases. It can have primary or secondary origin, and a wide range of sources. In the case of forest fires, in addition to the difficulty of representing primary PM emission from biomass burning, the inaccuracy of predicting secondary organic aerosol formation may play an important role in model performance. In summary, the calculated performance metrics indicate reasonable performance of the modelling system, supporting its usefulness to predict smoke transport and chemistry and delivering information to prevent human exposure to smoke.

**Table 4.** Performance metrics, calculated by comparing model results against monitoring station observations.

		NMB	RMSE	MFB	IOA	R	$\bar{O}$	NMB	RMSE	MFB	IOA	R	$\bar{O}$
		PM <sub>10</sub>						PM <sub>2.5</sub>					
D02 vs stations	Agia_paraskevi	0.53	101	0.11	0.17	0.15	44	1.12	76	0.44	0.20	0.22	24
	Aliartos <sup>^</sup>	0.64	174	0.06	0.25	<b>0.27</b>	63	0.63	131	0.17	<b>0.36</b>	<b>0.31</b>	48
	Koropi	0.40	89	<b>-0.06</b>	0.22	0.24	40						
	Lykovrisi	0.65	124	0.27	0.37	0.27	59						
	Nea_smirni	0.16	57	0.14	<b>0.38</b>	0.17	54						
	peristeri	0.17	65	0.06	0.34	0.10	61						
	Thrakomakedones	<b>-0.11</b>	<b>56</b>	-0.24	0.31	0.02	58	<b>0.18</b>	<b>37</b>	<b>0.04</b>	0.32	0.08	31
		CO						O <sub>3</sub>					
	Agia_paraskevi							-0.06	66	-0.34	0.67	0.70	112
	Aliartos <sup>^</sup>							0.65	109	0.41	0.54	0.68	95
	Koropi							<b>0.02</b>	<b>53</b>	-0.12	0.63	0.62	106
	Lykovrisi							0.21	59	0.09	<b>0.78</b>	0.67	91
	Nea_smirni	0.34	0.83	0.21	0.37	0.19	0.58	0.11	57	-0.43	0.78	<b>0.74</b>	82
	Peristeri							0.20	64	-0.14	0.75	0.72	87
	Thrakomakedones							0.07	68	<b>0.07</b>	0.62	0.35	145
		PM <sub>10</sub>						PM <sub>2.5</sub>					
D03 vs stations	Agia_paraskevi	0.43	112	<b>0.03</b>	0.17	0.18	44	0.96	82	0.35	0.23	0.29	24
	Aliartos <sup>^</sup>												
	Koropi	<b>-0.06</b>	<b>33</b>	-0.17	<b>0.57</b>	<b>0.40</b>	40						
	Lykovrisi	0.23	117	0.10	0.27	0.14	59						
	Nea_smirni	0.09	52	0.07	0.51	0.27	54						
	Peristeri	0.38	73	0.22	0.34	0.10	61						
	Thrakomakedones	-0.19	48	-0.32	0.46	0.22	58	<b>0.07</b>	<b>32</b>	<b>-0.06</b>	<b>0.51</b>	<b>0.28</b>	31
		CO						O <sub>3</sub>					
	Agia_paraskevi							<b>0.04</b>	54	-0.12	0.73	0.71	112
	Aliartos <sup>^</sup>							0.71	117	0.40	0.57	<b>0.79</b>	95
	Koropi							0.04	<b>48</b>	<b>-0.04</b>	0.63	0.57	106
	Lykovrisi							0.26	60	0.16	0.79	0.71	91
	Nea_smirni	0.48	0.98	0.10	0.52	0.37	0.58	0.17	64	-0.39	0.74	0.70	82
	Peristeri							0.04	54	-0.37	<b>0.80</b>	0.75	87
	Thrakomakedones							0.13	74	0.10	0.65	0.45	145

Values of stations with best performance are shown in bold.

<sup>^</sup>The Aliartos station is outside the D03 domain.

## Conclusions

The high spatiotemporal resolution of the calculated concentrations allowed a more detailed analysis of the smoke plume dispersion and development, which would be unmanageable with satellite images or local air-quality monitoring stations. The simulations compared well with the measurements in general. The performance metrics show that the computational

domain with 1 km resolution performed slightly better than that with 5 km resolution. For the finer domain, ozone had the highest index of agreement, with measurements ranging from 0.65 to 0.8 depending on the location, whereas for particulate matter, it ranged from 0.17 to 0.57. The mean fractional bias was of 3% for particulate matter and -4% for ozone.

The results show that all the studied locations around Athens had PM<sub>10</sub> and O<sub>3</sub> levels exceeding the values defined

by the European Commission for the protection of human health during the wildfire events, in particular on 5 August. The smoke cloud that settled over Athens on 6 August also led to extreme simulated hourly values of  $PM_{10} - 1152 \mu g m^{-3}$  in Lykovrisi.

The AERONET observations suggest that the smoke concentrations may have reached their peak on 7 August. This is supported by the simulation results, where an increasing trend is seen in  $PM_{10}$  concentrations at the end of 6 August. Based on obtained data and on the European legislation for the protection of the human health, it is likely that the low air quality during the event had a strong negative impact on human health.

## References

- Ager AA, Palaiologou P, Evers CR, Day MA, Ringo C, Short K (2019) Wildfire exposure to the wildland–urban interface in the western US. *Applied Geography* **111**, 102059. doi:10.1016/j.apgeog.2019.102059
- Aguilera R, Corringham T, Gershunov A, Benmarhnia T (2021) Wildfire smoke impacts respiratory health more than fine particles from other sources: observational evidence from southern California. *Nature Communications* **12**, 1493. doi:10.1038/s41467-021-21708-0
- Bessagnet B, Pirovano G, Mircea M, Cuvelier C, Aulinger A, Calori G, Ciarelli G, Manders A, Stern R, Tsyro S, García Vivanco M, Thunis P, Pay MT, Colette A, Couvidat F, Meleux F, Rouil L, Ung A, Aksoyoglu S, Baldasano JM, Bieser J, Briganti G, Cappelletti A, D'Isidoro M, Finardi S, Kranenburg R, Silibello C, Carnevale C, Aas W, Dupont JC, Fagerli H, Gonzalez L, Menut L, Prévôt ASH, Roberts P, White L (2016) Presentation of the EURODELTA III intercomparison exercise – evaluation of the chemistry transport models' performance on criteria pollutants and joint analysis with meteorology. *Atmospheric Chemistry and Physics* **16**, 12667–12701. doi:10.5194/acp-16-12667-2016
- Black C, Tesfaigzi Y, Bassein JA, Miller LA (2017) Wildfire smoke exposure and human health: Significant gaps in research for a growing public health issue. *Environmental Toxicology and Pharmacology* **55**, 186–195. doi:10.1016/j.etap.2017.08.022
- Cascio WE (2018) Wildland fire smoke and human health. *Science of the Total Environment* **624**, 586–595. doi:10.1016/j.scitotenv.2017.12.086
- Colette A, Andersson C, Manders A, Mar K, Mircea M, Pay MT, Raffort V, Tsyro S, Cuvelier C, Adani M, Bessagnet B, Bergström R, Briganti G, Butler T, Cappelletti A, Couvidat F, D'Isidoro M, Dombia T, Fagerli H, Granier C, Heyes C, Klimont Z, Ojha N, Otero N, Schaap M, Sindelarova K, Stegehuis AI, Roustan Y, Vautard R, van Meijgaard E, Vivanco MG, Wind P (2017) Eurodelta-trends, a multi-model experiment of air quality hindcast in Europe over 1990–2010. *Geoscientific Model Development* **10**, 3255–3276. doi:10.5194/gmd-10-3255-2017
- Corona P, Ascoli D, Barbati A, Bovio G, Colangelo G, Elia M, Garfi V, Iovino F, Laforteza R, Leone V, Lovreglio R, Marchetti M, Marchi M, Menguzzato G, Nocentini S, Picchio R, Portoghesi R, Puletti N, Sanesi G, Chianucci F (2015) Integrated forest management to prevent wildfires under Mediterranean environments. *Annals of Silvicultural Research* **39**, 1–22. doi:10.12899/asr-946
- D'Evelyn SM, Jung J, Alvarado E, Baumgartner J, Caligiuri P, Hagmann RK, Henderson SB, Hessburg PF, Hopkins S, Kasner EJ, Krawchuk MA, Krenz JE, Lydersen JM, Marlier ME, Masuda YJ, Metlen K, Mittelstaedt G, Prichard SJ, Schollaert CL, Smith EB, Stevens JT, Tessum CW, ReebWhitaker C, Wilkins JL, Wolff NH, Wood LM, Haugo RD, Spector JT (2022) Wildfire, smoke exposure, human health, and environmental justice need to be integrated into forest restoration and management. *Current Environmental Health Reports* **9**, 366–385. doi:10.1007/s40572-022-00355-7
- Dupuy JL, Fargeon H, Martin-StPaul N, Pimont F, Ruffault J, Guijarro M, Hernando C, Madrigal J, Fernandes P (2020) Climate change impact on future wildfire danger and activity in southern Europe: a review. *Annals of Forest Science* **77**, 35. doi:10.1007/s13595-020-00933-5
- Eck TF, Holben BN, Reid JS, Dubovik O, Smirnov A, O'Neill NT, Slutsker I, Kinne S (1999) Wavelength dependence of the optical depth of biomass burning, urban, and desert dust aerosols. *Journal of Geophysical Research: Atmospheres* **104**(D24), 31333–31349. doi:10.1029/1999JD900923
- ECMWF: European Centre for Medium-Range Weather Forecast (2022) ERA5 hourly data on pressure levels from 1979 to present. Copernicus Climate Change Service (C3S) Climate Data Store (CDS). [Accessed March 2022]
- EEA (2021) Air quality e-reporting. (European Environmental Agency) Available at <https://www.eea.europa.eu/data-and-maps/data/aqereporting-2> [retrieved January 2022]
- EFFIS (2022) Rapid Damage Assessment – MODIS Burnt Areas. (European Forest Fire Information System) Available at <https://effis.jrc.ec.europa.eu/about-effis/technical-background/rapid-damage-assessment>
- Elliott CT, Henderson SB, Wan V (2013) Time series analysis of fine particulate matter and asthma reliever dispensations in populations affected by forest fires. *Environmental Health* **12**, 11. doi:10.1186/1476-069X-12-11
- EMEP/Centre on Emission Inventories and Projections database (2021) EMEP gridding 2021/2019. Available at <https://webdab01.umweltbundesamt.at/download/gridding2021/2019/> [retrieved March 2022]
- Fernandes AP, Lopes D, Sorte S, Monteiro A, Gama C, Reis J, Menezes I, Osswald T, Borrego C, Almeida M, Ribeiro LM, Viegas DX, Miranda AI (2022) Smoke emissions from the extreme wildfire events in central Portugal in October 2017. *International Journal of Wildland Fire* **31**, 989–1001. doi:10.1071/WF21097
- Giannaros TM, Papavasileiou G, Lagouvardos K, Kotroni V, Dafis S, Karagiannidis A, Dragozi E (2022) Meteorological analysis of the 2021 extreme wildfires in Greece: lessons learned and implications for early warning of the potential for pyroconvection. *Atmosphere* **13**, 475. doi:10.3390/atmos13030475
- Giglio L, Hall JV, Schroeder W, Justice CO (2021) MODIS/Terra thermal anomalies/fire 5-min L2 swath 1km. doi:10.5067/MODIS/MOD14.NRT.061 [retrieved March 2021]
- Giles DM, Sinyuk A, Sorokin MG, Schafer JS, Smirnov A, Slutsker I, Eck TF, Holben BN, Lewis JR, Campbell JR, Welton EJ, Korokin SV, Lyapustin AI (2019) Advancements in the aerosol robotic network (AERONET) version 3 database – automated near-real-time quality control algorithm with improved cloud screening for sun photometer aerosol optical depth (AOD) measurements. *Atmospheric Measurement Techniques* **12**, 169–209. doi:10.5194/amt-12-169-2019
- Haikerwal A, Akram M, Monaco AD, Smith K, Sim MR, Meyer M, Tonkin AM, Abramson MJ, Dennekamp M (2015) Impact of fine particulate matter ( $PM_{2.5}$ ) exposure during wildfires on cardiovascular health outcomes. *Journal of the American Heart Association* **4**, e001653. doi:10.1161/JAHA.114.001653
- Haikerwal A, Akram M, Sim MR, Meyer M, Abramson MJ, Dennekamp M (2016) Fine particulate matter ( $PM_{2.5}$ ) exposure during a prolonged wildfire period and emergency department visits for asthma. *Respirology* **21**, 88–94. doi:10.1111/resp.12613
- Hellenic Fire Service (2021) Event log - forest fires 2021. Available at [https://www.fireservice.gr/en\\_US/synola-dedomenon](https://www.fireservice.gr/en_US/synola-dedomenon) [retrieved June 2022]
- Jaffe DA, Wigder NL (2012) Ozone production from wildfires: a critical review. *Atmospheric Environment* **51**, 1–10. doi:10.1016/j.atmosenv.2011.11.063
- Kukkonen J, Olsson T, Schultz DM, Baklanov A, Klein T, Miranda AI, Monteiro A, Hirtl M, Tarvainen V, Boy M, Peuch VH, Poupkou A, Kioutsioukis I, Finardi S, Sofiev M, Sokhi R, Lehtinen KEJ, Karatzas K, San José R, Astitha M, Kallos G, Schaap M, Reimer E, Jakobs H, Eben K (2012) A review of operational, regional-scale, chemical weather forecasting models in Europe. *Atmospheric Chemistry and Physics* **12**, 1–87. doi:10.5194/acp-12-1-2012
- Menut L, Flamant C, Turquety S, Deroubaix A, Chazette P, Meynadier R (2018) Impact of biomass burning on pollutant surface concentrations in megacities of the Gulf of Guinea. *Atmospheric Chemistry and Physics* **18**, 2687–2707. doi:10.5194/acp-18-2687-2018
- Menut L, Bessagnet B, Briant R, Cholakian A, Couvidat F, Mailler S, Pennel R, Siour G, Tuccella P, Turquety S, Valari M (2021) The CHIMERE v2020r1 online chemistry-transport model. *Geoscientific Model Development* **14**, 6781–6811. doi:10.5194/gmd-14-6781-2021

- Miranda AI, Amorim JH, Martins V, Pimentel C, Rodrigues R, Tavares R, Borrego C (2008) Numerical modelling of the impact of wildland-urban interface fires on Coimbra air quality. *WIT Transactions on Ecology and the Environment* **119**, 333–342. doi:10.2495/FIVA080331
- Miranda AI, Martins V, Cascão P, Amorim JH, Valente J, Tavares R, Borrego C, Tchepel O, Ferreira AJ, Cordeiro CR, Viegas DX, Ribeiro LM, Pita LP (2010) Monitoring of firefighters' exposure to smoke during fire experiments in Portugal. *Environment International* **36**, 736–745. doi:10.1016/j.envint.2010.05.009
- Miranda AI, Martins V, Cascão P, Amorim JH, Valente J, Borrego C, Ferreira AJ, Cordeiro CR, Viegas DX, Ottmar R (2012) Wildland smoke exposure values and exhaled breath indicators in firefighters. *Journal of Toxicology and Environmental Health, Part A* **75**, 831–843. doi:10.1080/15287394.2012.690686
- Péré JC, Bessagnet B, Mallet M, Waquet F, Chiappello I, Minvielle F, Pont V, Menut L (2014) Direct radiative effect of the Russian wildfires and its impact on air temperature and atmospheric dynamics during August 2010. *Atmospheric Chemistry and Physics* **14**, 1999–2013. doi:10.5194/acp-14-1999-2014
- Rappold AG, Reyes J, Pouliot G, Cascio WE, Diaz-Sanchez D (2017) Community vulnerability to health impacts of wildland fire smoke exposure. *Environmental Science & Technology* **51**, 6674–6682. doi:10.1021/acs.est.6b06200
- Rea G, Paton-Walsh C, Turquety S, Cope M, Griffith D (2016) Impact of the New South Wales fires during October 2013 on regional air quality in eastern Australia. *Atmospheric Environment* **131**, 150–163. doi:10.1016/j.atmosenv.2016.01.034
- Reid CE, Brauer M, Johnston FH, Jerrett M, Balmes JR, Elliott CT (2016) Critical review of health impacts of wildfire smoke exposure. *Environmental Health Perspectives* **124**, 1334–1343. doi:10.1289/ehp.1409277
- Schneider SR, Abbatt JPD (2022) Wildfire atmospheric chemistry: climate and air quality impacts. *Trends in Chemistry* **4**, 255–257. doi:10.1016/j.trechm.2021.12.004
- Schneider SR, Lee K, Santos G, Abbatt JPD (2021) Air quality data approach for defining wildfire influence: impacts on PM<sub>2.5</sub>, NO<sub>2</sub>, CO, and O<sub>3</sub> in western Canadian cities. *Environmental Science & Technology* **55**, 13709–13717. doi:10.1021/acs.est.1c04042
- Sebastião R, Sorte S, Valente J, Miranda AI, Fernandes JM (2019) Detecting changes in the heart rate of firefighters to prevent smoke inhalation and health effects. *Evolving Systems* **10**, 295–304. doi:10.1007/s12530-018-9241-0
- Smith H (2021) 'Apocalyptic' scenes hit Greece as Athens besieged by fire. *The Guardian*, 7 August 2021. Available at <https://www.theguardian.com/world/2021/aug/07>
- Sofiev M, Ermakova T, Vankevich R (2012) Evaluation of the smoke injection height from wildland fires using remote-sensing data. *Atmospheric Chemistry and Physics* **12**, 1995–2006. doi:10.5194/acp-12-1995-2012
- Turquety S, Menut L, Siour G, Mailler S, Hadji-Lazaro J, George M, Clerbaux C, Hurtmans D, Coheur PF (2020) Apiflamev2.0 biomass burning emissions model: impact of refined input parameters on atmospheric concentration in Portugal in summer 2016. *Geoscientific Model Development* **13**, 2981–3009. doi:10.5194/gmd-13-2981-2020
- Valente J, Miranda AI, Lopes AG, Borrego C, Viegas DX, Lopes M (2007) Local-scale modelling system to simulate smoke dispersion. *International Journal of Wildland Fire* **16**, 196–203. doi:10.1071/WF06085
- Veira A, Kloster S, Wilkenskjeld S, Remy S (2015) Fire emission heights in the climate system – part 1: Global plume height patterns simulated by ECHAM6-HAM2. *Atmospheric Chemistry and Physics* **15**, 7155–7171. doi:10.5194/acp-15-7155-2015
- Wettstein ZS, Hoshiko S, Fahimi J, Harrison RJ, Cascio WE, Rappold AG (2018) Cardiovascular and cerebrovascular emergency department visits associated with wildfire smoke exposure in California in 2015. *Journal of the American Heart Association* **7**, e007492. doi:10.1161/JAHA.117.007492
- WHO (1999) 'Health guidelines for vegetation fire events.' (World Health Organization: Geneva, Switzerland)
- Xanthopoulos G, Athansasiou M, Kaoukis K (2022) Suppression versus prevention: the disastrous forest fire season of 2021 in Greece. *Wildfire, Quarter 2*, 18–24.
- Xu Q, Westerling AL, Notohamiprodjo A, Wiedinmyer C, Picotte JJ, Parks SA, Hurteau MD, Marlier ME, Kolden CA, Sam JA, Baldwin WJ, Ade C (2022) Wildfire burn severity and emissions inventory: an example implementation over California. *Environmental Research Letters* **17**, 085008. doi:10.1088/1748-9326/ac80d0
- Yang Z, Demoz B, Delgado R, Sullivan J, Tangborn A, Lee P (2022) Influence of the transported Canadian wildfire smoke on the ozone and particle pollution over the mid-Atlantic United States. *Atmospheric Environment* **273**, 11894. doi:10.1016/j.atmosenv.2022.118940
- Yao J, Eyamie J, Henderson SB (2016) Evaluation of a spatially resolved forest fire smoke model for population-based epidemiologic exposure assessment. *Journal of Exposure Science & Environmental Epidemiology* **26**, 233–240. doi:10.1038/jes.2014.67

**Data availability.** The data that support this study will be shared on reasonable request to the corresponding author.

**Conflicts of interest.** The authors declare no conflicts of interest.

**Declaration of funding.** The authors are grateful for the financial support of the Foundation for Science and Technology, IP, through national funds, under the SmokeStorm project (PCIF/MPG/0147/2019), contract grant for C. Gama (2021.00732.CEECIND) and PhD Studentship to T. Osswald (2022.10992.BD), and CESAM (UIDP/50017/2020 + UIDB/50017/2020 + LA/P/0094/2020). The authors also acknowledge the financial support of the FirEUriSk project, which receives funding from the European Union's Horizon 2020 Research and Innovation Programme under grant agreement No. 101003890.

**Acknowledgements.** We acknowledge the CHIMERE and APIFLAME developer teams for the free use of their models. We also acknowledge the AERONET network, in particular Alex Papayannis and Vassilis Amiridis for their effort in establishing and maintaining the AERONET sites of the National Technical University of Athens (ATHENS\_NTUA) and the National Observatory of Athens (ATHENS-NOA), and the EEA for the freely downloadable air quality station data provided.

#### Author affiliations

<sup>A</sup>Centre for Environmental and Marine Studies (CESAM) and Department of Environment and Planning, Campus Universitário de Santiago, University of Aveiro, 3810-193 Aveiro, Portugal.

<sup>B</sup>Center for Security Studies (KEMEA), 4 P. Kenellopoulou str., GR-101 77 Athens, Greece.